Stoch Environ Res Risk Assess (2017) 31:2627–2643
DOI 10.1007/s00477-016-1349-9

ORIGINAL PAPER

Regional response of runoff in CMIP5 multi-model climate projections of Jiangsu Province, China

Zhiyong Wu[1] · Xia Chen[2] · Guihua Lu[1] · Heng Xiao[3] · Hai He[1] · Jianhua Zhang[4]

Published online: 9 November 2016
© Springer-Verlag Berlin Heidelberg 2016

Abstract Surface runoff is a major water resource component and its spatial and temporal variations significantly impact on regional socio-economic development. In this study, changes to surface runoff in Jiangsu Province, China, were simulated using the variable infiltration capacity (VIC) model for the period 2011–2040, using input data from five Coupled Model Intercomparison Project Phase 5 (CMIP5) climate models and three different Representative Concentration Pathway (RCP) scenarios. In general, annual mean precipitation under the five models and three scenarios showed a fluctuating upward trend, while annual mean temperatures were projected to increase by up to 1.34 °C, as compared with the reference period (1970–1999). Monthly mean runoff depths were generally predicted to increase, with the most significant increases occurring in December. Increasing runoff depths were highest under the RCP8.5 emission scenario and lowest under RCP4.5. The results of this study provide an important reference for policymakers planning for the future water resources in Jiangsu Province. Furthermore, we conducted a case study with the VIC model and it showed high consistency with gauges and provides a new reference for the studies of other plain regions.

Keywords Jiangsu Province · Climate change · Surface runoff · CMIP5 · Variable infiltration capacity model

✉ Zhiyong Wu
wzyhhu@gmail.com

[1] College of Hydrology and Water Resources, Hohai University, No.1 Xikang Road, Nanjing, Jiangsu Province, China

[2] School of Business, Hohai University, No.8 Focheng West Road, Nanjing, Jiangsu Province, China

[3] School of Water Conservancy, North China University of Water Resources and Electric Power, Zhengzhou, Henan Province, China

[4] Jiangsu Provincial Department of Water Resources, Nanjing, Jiangsu Province, China

1 Introduction

Global climate change has resulted in increasingly significant and far-reaching impacts and is a major issue of concern for the international community (Sivakumar 2011; Gosling et al. 2011; Kusangaya et al. 2014). Climate change exacerbates processes within global and regional hydrological cycles, resulting in changes to atmospheric circulation and ice conditions. Consequent changes in precipitation, evaporation, soil moisture, and river runoff, ultimately lead to the spatial and temporal re-allocation of water resources (Li et al. 2010). The fifth assessment report by the Intergovernmental Panel on Climate Change (IPCC) showed that, since 1901, mean precipitation over land areas of the northern mid-latitudes has increased, while between 1880 and 2012, the global mean surface temperature has risen by 0.85 °C (IPCC 2013). These changes will significantly affect temperature, precipitation and runoff; thus, causing an increase in flooding, droughts and other extreme events (Wu et al. 2010; Vaghefi et al. 2014; Spinoni et al. 2015; Wang et al. 2015a).

Jiangsu Province, which is a typical northern mid-high latitude plain area, covers a total area of 102,600 km^2, of which 70,000 km^2 represent downstream plains of the rivers. Owing to its moderate geographical and climatic conditions, the province represents the second largest economic region in China. The availability of water resources has been an important factor in the sustained

economic development of Jiangsu Province (Ma 2007); however, as the area is located in both the north–south climate transition zone and in the marine–terrestrial transition zone, it is extremely sensitive to climate change. Weather and climate related disasters occur frequently and as such the spatial and temporal distribution of water resources is uneven and annual variations are large (Yang and Li 2003; Liu et al. 2009; Sun et al. 2013a; Xia et al. 2014). To date, climate change in Jiangsu Province has primarily affected precipitation (Deng et al. 2004; Qiu et al. 2008; Fu et al. 2013).

Rainfall levels determine the total water budget involved in the land surface water cycle, and variations reflect regional changes in water resources (Gu et al. 2010). In contrast, river runoff is related to social water needs (e.g., irrigation) more directly. Extreme events that affect runoff (e.g., flooding or droughts) can threaten economic development and human safety (Madsen et al. 2014; Tezuka et al. 2014; Wang et al. 2015b). Therefore, the most appropriate approach to assessing regional water issues is from the perspective of runoff. However, few studies have focused on runoff in Jiangsu Province, while fewer still have considered the impact on runoff based on future climate change scenarios. This is due to the lack of closed basins within the region, which significantly complicates the calibration of parameters during the building of hydrological models for plain areas. Climate models are the main tool used to project climate change (Dufresne et al. 2013), while the evaluation of climate change impacts on regional runoff usually involves a nested climate model and hydrological model approach (Wang and Zhan 2015). In this study, we simulated the impact of future climate change on runoff in Jiangsu Province by setting up a method to determine variable infiltration capacity (VIC) large-scale hydrological model parameters for plains, constructing a VIC model for Jiangsu Province, and by nesting multiple Coupled Model Intercomparison Project Phase 5 (CMIP5) climate models under the latest IPCC Representative Concentration Pathway (RCP) emission scenarios. The results of this study will provide support for water resources planning and the sustainable social and economic development of the region.

2 Data and methods

2.1 Study area

Jiangsu Province is located along the eastern coast of China (116.3°–121.95°E, 30.75°–35.33°N) and is an important part of the Yangtze River Delta region (Fig. 1). The terrain mainly consists of plains (having a higher terrain area than any other province in China), which cover an area of

Fig. 1 The location of Jiangsu Province, meteorological stations, rain gauge stations, soil moisture station (Xuzhou Station) and 13 cities. *XZ* Xuzhou, *LYG* Lianyungang, *SQ* Suqian, *HA* Huai'an, *YC* Yancheng, *YZ* Yangzhou, *TZ* Taizhou, *NJ* Nanjing, *ZJ* Zhenjiang, *NT* Nantong, *CZ* Changzhou, *WX* Wuxi, *SZ* Suzhou

70,000 km^2, accounting for more than 70% of the area of Jiangsu Province. Jiangsu is the lowest-lying province in China, with the altitude of most areas being less than 50 m. Hills, which are concentrated in the southwest, account for just 14.3% of the total area. Jiangsu is located downstream of the Jianghuai and Yishusi rivers, while the Yangtze River runs across the southern part of the province. The Taihu, Hongze and Luoma lakes, along with other medium-sized lakes, are all located in Jiangsu, as are the Grand Canal, Tongyu Canal and other tributary rivers. Jiangsu experiences a temperate to subtropical transitional climate and moderate rainfall. Taking the Huaihe River as the boundary, the northern part of the province experiences a warm, humid and semi-humid monsoon climate, while the south experiences a subtropical humid monsoon climate. The mean temperature ranges between 13 and 16 °C, and gradually increases from northeast to southwest. Jiangsu is rich in water resources and the annual runoff is between 150 mm and 400 mm.

2.2 Meteorological data

Meteorological data was provided by the China Meteorological Data Sharing Network (http://www.escience.gov.cn/metdata/page/index.html) and the Jiangsu Province Hydrology and Water Resources Investigation Bureau (The office of Jiangsu province water resource comprehensive planning leading group 2014). Daily temperature and precipitation data were from 32 meteorological stations and 81 rain gauge stations during 1956–2011. We used the inverse

distance weighting method (Lu and Wong 2008; Chen and Li 2012) to interpolate the site data across Jiangsu province into a 0.125°×0.125° horizontal resolution grid.

2.3 Emissions scenarios

Greenhouse gas emissions scenarios are the basis for global and regional climate predictions, and are usually calculated according to a series of assumptions (e.g., population growth, economic development, technological advances, environmental conditions, globalization, and fairness) that correspond to different social and economic development projections. In this study, we used three emission scenarios identified as major future climate change scenarios (Xu and Xu 2012): the high emission RCP8.5 scenario, the medium emission RCP4.5 scenario, and the low emission RCP2.6 scenario (IPCC 2012). RCP8.5 assumes a high population, low technological innovation, slow energy improvement, and slow income growth, all leading to a prolonged high-energy demand, high greenhouse gas emissions, a lack of policy response to climate change, and a predicted radiative forcing of 8.5 W/m^2 in 2100. In contrast, RCP4.5 predicts that radiative forcing will stabilize at 4.5 W/m^2 in 2100, while in RCP2.6 there is a limited global mean temperature rise of 2.0 °C, post-21st century energy applications for negative emissions, a radiative forcing peak before 2100, and a subsequent reduction in radiative forcing to 2.6 W/m^2 in 2100.

2.4 Methods

2.4.1 Climate model filter

The climate models used in this study were chosen based on the long-term historical climate data from 47 CMIP5 models simulated under RCP2.6, RCP4.5, and RCP8.5. The spatial resolutions of the original data in each model were different; therefore, we took a reference period (1970–1999) and used it for comparison with the forecast climate data in this study (2011–2040). Considering the output results of GCM are grid data, we selected bilinear interpolation (Li et al. 2000) to unify the data onto the Jiangsu Province 1°×1° grid. In order to reduce the uncertainty of climate models and projections of climate change, the equidistant quantile matching method (Lu et al. 2014) was applied to revise multi-model ensemble mean monthly data, and then we applied the Delta method (Zorita and von 1999) to generate daily data for the reference period and three future scenarios.

To reduce model uncertainty and select the most appropriate approach (Zhang et al. 2010), we first evaluated the 47 CMIP5 global climate models (GCMs) by comparing the relative error between the simulated mean precipitation of the region across the reference period (1970–1999) and the mean measured precipitation, and the absolute error between the simulated mean temperature and the mean measured temperature (Table 1). It showed that the various models all well simulated the observed precipitation and temperature in Jiangsu province. While CMCC-CESM showed significant errors in precipitation, that of the other models was approximately +50%. For temperature, CNRM-CM5 showed significant error, but that of all other models was approximately +3 °C. We also calculated the correlation of precipitation and temperature of 47 models (Fig. 2). As we can see that the temperature of 47 models had a well correlation to measured data in the reference period, but there was fluctuation in correlation of precipitation between 0.951 and 0.997.

Since the parameterization process of many models are the same or belonging to the same category, it may lead to some similarities between results of these models and the number of models with consistent results may not be fully representative of the credibility and reliability of the conclusions (Zhao et al. 2013). If all these models in this agency are chosen, it certainly will bring about greater deviation on estimation of future climate change and runoff. Therefore, we chose hierarchical clustering analysis method (Pennell 2010) to select relatively independent models based on the independence between models of precipitation simulation. Specific steps are as follows:

1. Calculate errors between annual average simulated and observed values in every grid point (n) and each model (m), and normalize by the standard deviation (σ) of observed values to get single-model error $e_{n,m}$:

$$e_{n,m} = \left(f_{n,m} - o_n\right)/\sigma_n \quad (1)$$

   where, f represents the value of model simulation; o represents the observed value; $n=1,2,\ldots, N$, N represents grid points of covering the area; $m=1,2, \ldots, M$, M represents the amount of models. $e_{n,m}$ could be showed by vector quantity in space, $\mathrm{e}_m = (e_{1,m}, e_{2,m}, \cdots, e_{N,m})$.
2. Calculate multi-model average error $\bar{e}$:

$$\bar{e} = \frac{1}{M}\sum_{m=1}^{M} e_m \quad (2)$$

3. Eliminate affection of errors $\bar{e}$, and get error vector d_m:

$$\mathbf{d}_m = \mathbf{e}_m^* - r \cdot \bar{\mathbf{e}} \quad (3)$$

   where, $(\cdot)^*$ is vector after standardization; r is correlation coefficient of m and $\bar{e}$. After eliminate $\bar{e}$, pertinence of m and $\bar{e}$ is 0.
4. Calculate correlation coefficient matrix $r_{i,j}$, take gradation cluster analysis:

Table 1 Precipitation and temperature error in CMIP5 global climate models

N°	Model	Precipitation (mm/day)	Relative error (%)	Mean temperature (°C)	Absolute error (°C)
M01	ACCESS1-0	3.18	15.8	13.8	−1.3
M02	ACCESS1-3	3.66	33.4	13.9	−1.2
M03	bcc-csm1-1	3.3	20.2	13.7	−1.4
M04	bcc-csm1-1-m	2.45	−10.7	14.2	−0.9
M05	BNU-ESM	3.72	35.5	13.9	−1.3
M06	CanCM4	3.4	23.8	16.7	1.6
M07	CanESM2	3.24	18	17.1	2
M08	CCSM4	3.49	26.9	14.3	−0.8
M09	CESM1-BGC	3.47	26.4	14.4	−0.7
M10	CESM1-CAM5	3.7	34.5	14.1	−1.1
M11	CESM1-FASTCHEM	3.33	21.2	14.5	−0.6
M12	CESM1-WACCM	3.76	36.8	16.4	1.3
M13	CMCC-CESM	4.46	62.3	14.4	−0.7
M14	CMCC-CM	3.85	40.3	13.9	−1.2
M15	CMCC-CMS	3.9	41.8	14.7	−0.4
M16	CNRM-CM5	3	9.1	10.9	−4.2
M17	CSIRO-Mk3-6-0	2.56	−7	14.0	−1.1
M18	EC-EARTH	2.66	−3.1	14.5	−0.6
M19	FGOALS-g2	2.4	−12.5	12.9	−2.2
M20	FGOALS-s2	2.97	8.2	18.0	2.9
M21	FIO-ESM	3.53	28.4	15.3	0.2
M22	GFDL-CM2p1	2.9	5.4	12.8	−2.4
M23	GFDL-CM3	3.01	9.6	12.3	−2.8
M24	GFDL-ESM2G	2.6	−5.5	13.5	−1.6
M25	GFDL-ESM2 M	2.83	3.1	12.9	−2.2
M26	GISS-E2-H	2.84	3.6	15.1	0
M27	GISS-E2-H-CC	3.01	9.7	14.9	−0.2
M28	GISS-E2-R	2.84	3.4	15.6	0.5
M29	GISS-E2-R-CC	2.72	−1	15.7	0.6
M30	HadCM3	2.68	−2.4	13.6	−1.5
M31	HadGEM2-AO	2.77	0.7	14.7	−0.4
M32	HadGEM2-CC	2.57	−6.6	13.9	−1.2
M33	HadGEM2-ES	2.74	−0.2	14.2	−0.9
M34	inmcm4	3.69	34.3	11.3	−3.8
M35	IPSL-CM5A-LR	2.75	0	13.3	−1.8
M36	IPSL-CM5A-MR	2.74	−0.4	14.5	−0.6
M37	IPSL-CM5B-LR	2.59	−5.7	12.2	−2.9
M38	MIROC4 h	3.36	22.1	16.6	1.5
M39	MIROC5	3.26	18.6	16.7	1.5
M40	MIROC-ESM	2.89	5.3	16.5	1.4
M41	MIROC-ESM-CHEM	2.76	0.5	16.6	1.5
M42	MPI-ESM-LR	3.06	11.3	15.2	0.1
M43	MPI-ESM-MR	3.25	18.3	15.1	0
M44	MPI-ESM-P	3.07	11.9	15.2	0.1
M45	MRI-CGCM3	2.02	−26.3	13.9	−1.3
M46	NorESM1-M	3.43	25	13.3	−1.9
M47	NorESM1-ME	3.41	24.2	13.4	−1.8

Data based on comparison between modeled values (using Coupled Model Intercomparison Project Phase 5 models; CMIP5) and measured values of mean precipitation and temperature averaged over the reference period (1970−1999)

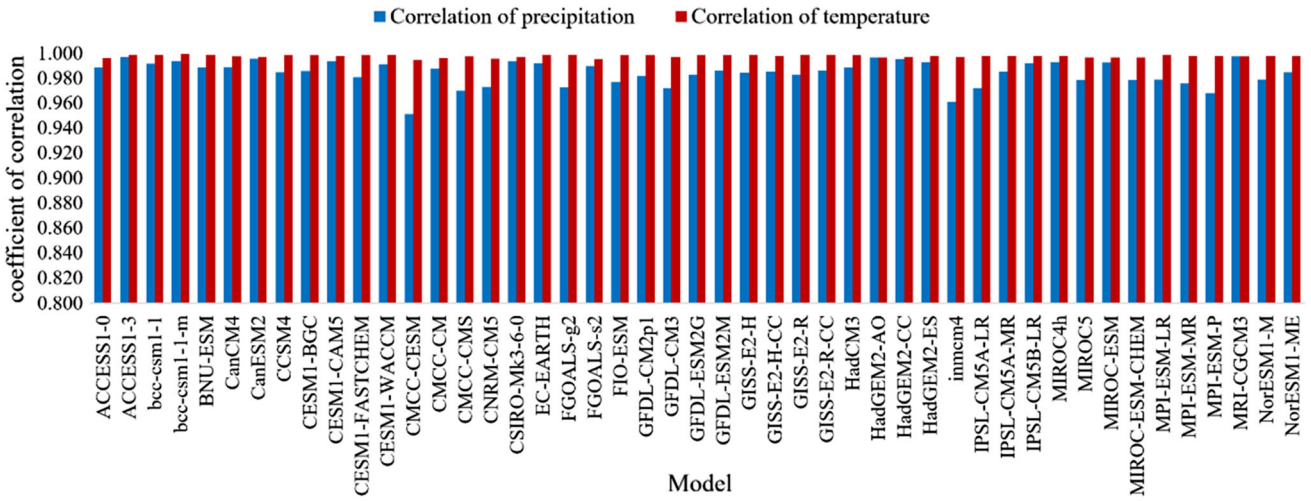

Fig. 2 Correlations of annual precipitation (*blue bars*) and temperature (*red bars*) of 47 models over Jiangsu province in reference period (1970–1999)

$$r_{i,j} = corr\left(\mathrm{d}_i, \mathrm{d}_j\right) \tag{4}$$

where, $i,j = 1, 2, \ldots, M$. we got average correlation coefficient matrix for four seasons $r_{i,j}$ according to the above steps, and used the weighted pair-wise average distance algorithm in Interactive Data Language(IDL) program language to take gradation cluster analysis. Considering the similarity of precipitation simulation results, hierarchical cluster analysis was selected to divide 47 models into five categories; and the most representative models from each category are selected according to their best simulation results of the current climate. Suppose these representative models which were relatively independent reflect the level of various types of model group in basin precipitation simulation. The result was shown in Fig. 3.

Of the 47 models, the 5 models chosen in this study were CCSM4, CSIRO-Mk3-6-0, GISS-E2-R, HadGEM2-ES, and IPSL-CM5A-LR (Table 2). For these models, the error in mean precipitation ranged between −7.0 and 26.9%. Simulations were more accurate for the summer and autumn, and showed greater uncertainty for spring and winter. The simulation error for annual mean temperature was small and ranged between −1.8 and 0.5 °C. With regard to season, the temperature simulation under GISS-E2-R had a positive bias, while the other four models had negative bias.

Furthermore, according to the correlation analysis results of Fig. 2, we got the correlation of five representative models (Table 3). As can be seen from the data in the table, the precipitation of five models had a well correlation with the gauges and the correlation of temperature was very good.

We also analyzed the cumulative distribution functions (CDF) of 47 models (Fig. 4). As shown in Fig. 4a, monthly precipitation of 47 models was between 3.54 and 4.78 mm, and that of five representative models was between 3.54 and 4.78 mm at 25% probability. Monthly precipitation of 47 models was between 1.46 and 3.94 mm, and that of five representative models was between 1.84 and 2.72 mm at 50% probability. Monthly precipitation of 47 models was between 0.65 and 2.51 mm, and that of five representative models was between 0.81 and 1.58 mm at 75% probability. Figure 4b shows that monthly temperature of 47 models was between 17.84 and 24.06 °C, and that of five representative models was between 19.86 and 21.13 °C at 25% probability. Monthly temperature of 47 models was between 11.31 and 18.13 °C, and that of five representative models was between 13.30 and 15.59 °C at 50% probability. Monthly temperature of 47 models was between 4.16 and 12.12 °C, and that of five representative models was between 6.73 and 10.65 °C at 75% probability. As we can see in the above figures, five representative models included models which were close to measured data and models which can reflect change intervals of 47 models, and it reflected the variation range of 47 models as a whole.

2.4.2 Setup and validation of the VIC model

Numerous hydrological models have been developed for impact assessment studies (Xu et al. 2008; Sun et al. 2013b; Lespinas et al. 2014), with the VIC model being one of the most widely used (Chang et al. 2014). The VIC model is a gridded large-scale hydrological model, in which each grid independently follows the energy balance and water balance in order to simulate hydrological and

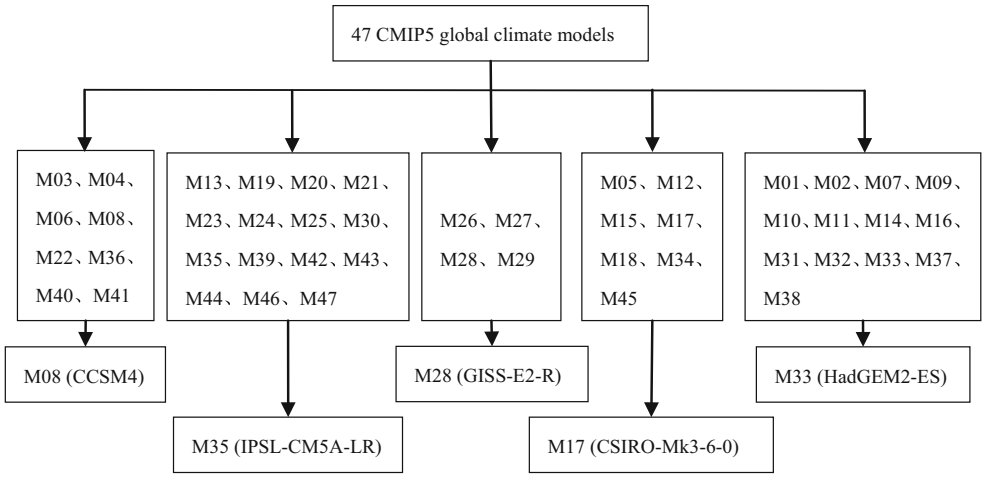

Fig. 3 Cluster analysis results and adopted models for the 47 Coupled Model Intercomparison Project Phase 5 (CMIP5) global climate models

Table 2 Climate model simulation results (2011−2040)

Model	Precipitation (%)					Temperature (°C)				
	Yr.	Spr.	Sum.	Aut.	Win.	Yr.	Spr.	Sum.	Aut.	Win.
CCSM4	26.9	107.4	0.5	12.4	17.3	−0.8	−0.1	0.0	−1.1	−2.1
CSIRO-Mk3-6-0	−7.0	24.2	−12.1	−21.4	−19.6	−1.1	−0.3	−1.2	−1.0	−1.9
GISS-E2-R	3.4	67.7	−31.4	−8.6	69.8	0.5	0.6	−1.5	0.2	2.7
HadGEM2-ES	−0.2	32.4	−22.9	−17.8	83.7	−0.9	−0.5	−1.1	−0.7	−1.2
IPSL-CM5A-LR	0.0	54.9	−19.4	−34.8	51.2	−1.8	−1.4	−1.1	−1.8	−3.0

Yr. year, *Spr.* spring, *Sum.* summer, *Aut.* autumn, *Win.* winter

Table 3 Correlation of five representative models between the GCM model outputs and measurements

Model	Correlation of precipitation	Correlation of temperature
CCSM4	0.985	0.998
CSIRO-Mk3-6-0	0.994	0.997
GISS-E2-R	0.982	0.999
HadGEM2-ES	0.993	0.998
IPSL-CM5A-LR	0.972	0.998

physical processes. Its most important feature is the introduction of the storage capacity curve concept of the Xin'anjiang model (Shu et al. 2008), which describes the uneven distribution of sub-grid soil moisture. Liang et al. (1996) explained the model principles in detail.

The parameters of VIC model can be divided into four categories: geography, vegetation, soil and hydrological. The first three are determined when the model is built and remain constant. However, due to the complexity of watershed runoff, it is difficult to determine hydrological parameters directly and so these must be calibrated using the measured hydrological data of each individual basin. The unique climate and geography of Jiangsu imposes new requirements for determining hydrological parameters. As few closed basins are available to verify the hydrological model, it is difficult to calibrate hydrological parameters by site-measured data. Formulas used to determine the hydrological parameters have typical national wide parameter transfer formula (NPTF) (Lu et al. 2010) and southern part of China parameter transfer formula (SPTF) (Lu et al. 2013).

NPTF is a hydrological gridding parameter formula that is based on nationwide 43 typical basins, established by structuring multiple regression equation using hydrological parameter, basin soil and climate factors. 43 typical basins were selected over different climatic regions in China, and they were divided into two sections. The first part was 35 basins which are used to calibrate hydrological parameter and establish hydrological parameter formula; the other 8 basins were used to verify the formula to ensure the independence of the basin. 17 factors of soil and climate in the basin were chosen to build the multiple regression

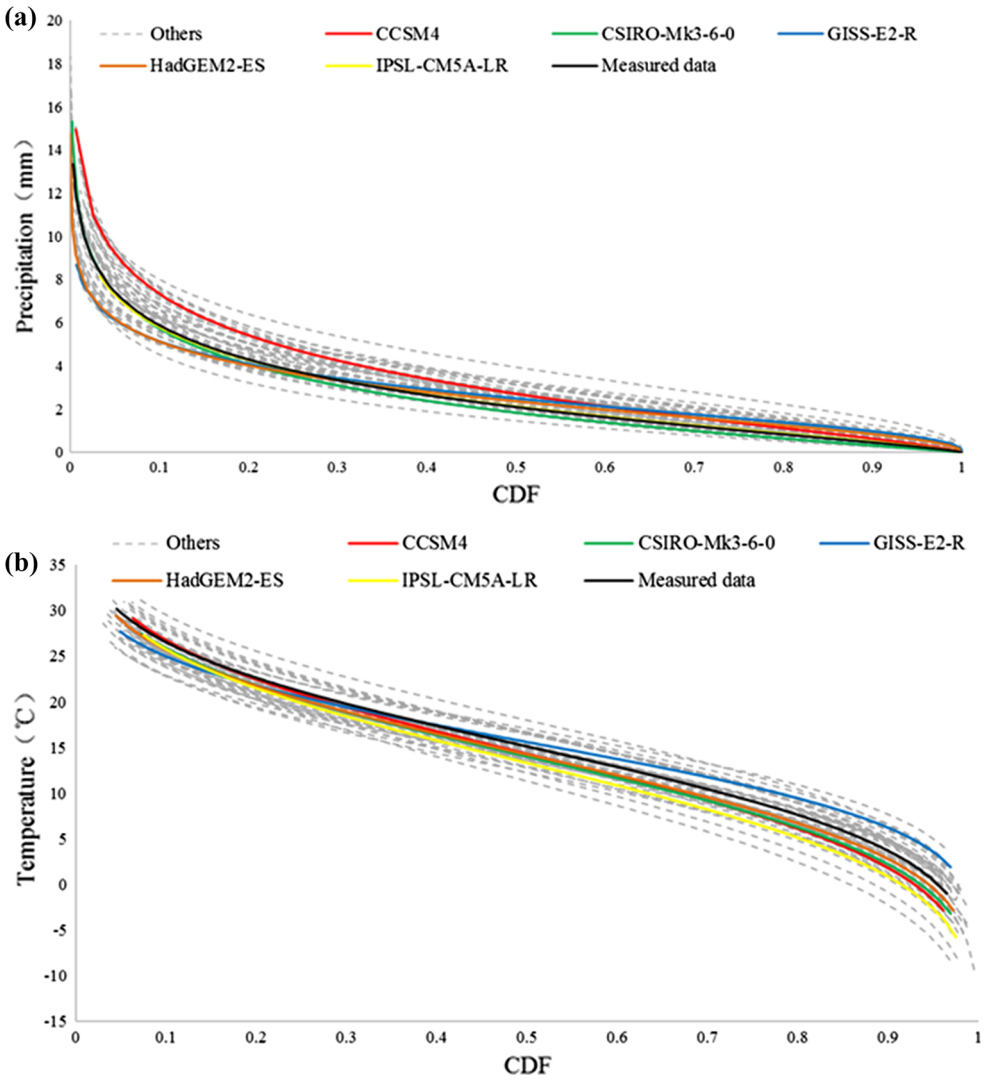

Fig. 4 The CDFs of average monthly precipitation (**a**) and temperature (**b**) of measured (*black solid*) and 47 models (*color solid* and *grey dashed*) data over Jiangsu province in reference period (1970–1999). The color solid lines represent five models (CCSM4, CSIRO-Mk3-6-0, GISS-E2-R, HadGEM2-ES, and IPSL-CM5A-LR), the grey dashed lines represent the other models

equation through stepwise regression. Three kinds of regression models were considered in regression analysis: multivariate linear regression model (LIN), multivariate square root model (SQRT), and multivariate logistic model (LOG). The optima land the most significant model was finally selected as the parameter formula. SPTF aims to rebuild gridding parameters formula in southern China because NPTF doesn't consider the impact of the special climate, soil and other factors in north-south differences and some factors like landform and vegetation feature. This formula was established based on 49 typical basins and 25 factors of climate, soil, vegetation and landform which are selected from south areas of China, then the VIC model hydrological gridding parameter formula was established in southern China. The multiple regression hydrological gridding parameter formula was built through stepwise regression, it can improve the nationwide VIC model gridding parameter formula and enhance VIC model simulation precision.

However, typical basins of these two sets of formula are not found in Jiangsu Province as they generally represent mountainous watershed. Parameters for use in plain areas require further testing and cannot be directly selected. Therefore, in this study, we used two sets of gridding formula (NPTF and SPTF) to calculate hydrological parameters (Table 4); however, we used rational analysis and fine-tuning to determine the exact parameters used, which were verified by comparison with data from the Jiangsu Water Resources Bulletin (JWRB). The hydrological parameters estimated, which varied spatially (Fig. 5), were as follows:

1. B represents the saturated water content capacity curve, which acts on D1 (0.1 m) and D2, and has a great impact on runoff. In Jiangsu Province the differences between topography and vegetation on the 0.125° × 0.125° grid is small; therefore, we chose NPTF for the initial calculation and did fine-tuning.

2. Ds represents the proportion of the maximum daily base flow when base flow non-linear growth occurs. This parameter is related to soil texture, and considering the low-lying topography of Jiangsu, lateral flow is slow, we chose the relatively small NPTF for the initial calculation.
3. Dsmax represents the base flow of the maximum daily flow. Again, given the low-lying topography of Jiangsu, lateral flow is slow; therefore, we chose the relatively small SPTF for the initial calculation and we performed fine-tuning.
4. Ws represents the proportion of underlying soil moisture and the maximum soil moisture when base flow nonlinear growth occurs. Because of the low-lying topography, groundwater outflow in the region is mostly smooth and linear, with nonlinear outflow rare; therefore, Ws was set to 1.
5. D2 represents the thickness of the second layer of the soil. Research in the Qinhuai River Basin of Jiangsu Province showed that the surface soil moisture content in fields around the Yangtze River ranged between 120 and 150 mm, while saturated water contents ranged

Table 4 Mean regional hydrological parameters calculated by NPTF and SPTF

Hydrological parameter	B[a]	Ds	Dsmax (mm/day)	Ws	D2 (m)	D3 (m)
Calculated by NPTF	0.062	0.090	16.576	0.832	0.976	0.485
Calculated by SPTF	0.216	0.139	6.532	0.921	0.204	0.298
Adopted	0.071	0.093	5.419	1.000	0.245	0.501

[a] B = saturated water content capacity curve; Ds = proportion of the maximum daily base flow when base flow non-linear growth occurs; Dsmax = base flow during maximum daily flow; D2 = the thickness of the second layer of the soil; D3 = the thickness of the third layer of the soil

NPTF National wide parameter transfer formula, *SPTF* Southern part of China parameter transfer formula

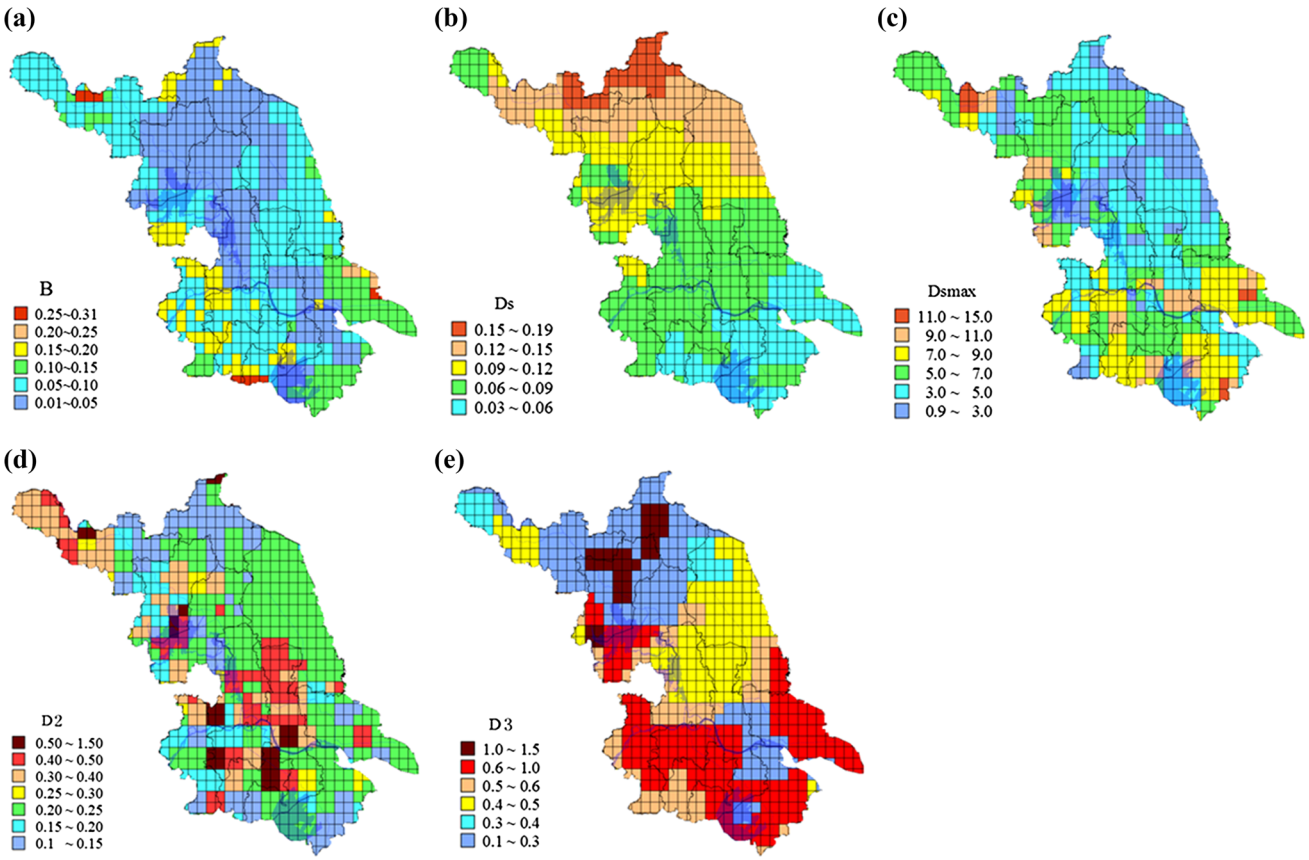

Fig. 5 The distribution of five hydrological parameters of VIC over Jiangsu Province with a 0.125°×0.125° resolution: **a** B (saturated water content capacity curve); **b** Ds (the proportion of the maximum daily base flow when base flow non-linear growth occurs); **c** Dsmax (base flow during maximum daily flow); **d** D2 (the thickness of the second layer of the soil); **e** D3 (the thickness of the third layer of the soil)

between 160 and 200 mm. Soil porosity, as calculated based on soil properties, was 0.49, and the effective soil thickness was 0.32–0.40. This thickness corresponds to D1 + D2 in the VIC model; therefore, the appropriate range for D2 was 0.22–0.30, and we selected SPTF for the initial calculation and then performed fine-tuning.

6. D3 represents the thickness of the third layer of the soil. In Jiangsu, the mean groundwater depth is 1–2 m; therefore, we selected NPTF for the initial calculation and then made appropriate adjustments.

The annual runoff of Jiangsu Province from 1956 to 2009, as modeled by the VIC, was similar to the measured values published by JWRB (Fig. 6). The mean values were 265 and 262 mm, respectively, while the relative error was only −1.4%; however, the data simulated by VIC was smaller than that published by JWRB. Both datasets fit well with annual discharge processes and their coefficient of determination came to 0.88. The annual mean absolute relative error was 18%, but there were 6 drought years (1978, 1994, 1966, 1967, 1973 and 1976) in which relative error was greater than 40%. The main reason for these significant differences was that the calculation methods of the VIC model for rainfall-runoff transformation relations in dry years was different from that used by the JWRB. The VIC model shares the storage capacity curve concept with the Xin'anjiang model, it assumes that precipitation fulfills interception vegetation firstly, and then all the rest are used to calculate runoff. The VIC model separates water source when calculating runoff, the upper layer soil produces direct runoff and upper and lower soil water infiltration, while the subsoil generates base flow. While in JWRB, the Jiangsu underlying is divided into Plains and mountains, and then according to land attribute is subdivided into construction land, water area and agricultural land (includes paddy field and dryland). The analysis was separately carried out from construction land, water area, paddy field and dryland according to their runoff characteristics.

At the same time, the process of soil moisture (0–100 cm) of Xuzhou station, Jiangsu province during 1981–1999 (Fig. 7) simulated by VIC model showed a good agreement between the simulated and measured soil moisture. The average value of measured data was 328 mm and that of simulated data was 316 mm, the relative error was −3.72%, and the coefficient of determination was 0.52. To verify the simulation of VIC model in space, we compared the annual runoff simulated by VIC and that in each city from Jiangsu province published by Jiangsu Water Resources Bulletin during 1980–2000 (Fig. 8). When we calculated the surface runoff of 13 cities, we first calculated the proportion of the grid in each region based on GIS tools, and then computed the average runoff depth of the region using the area ratio weighting method. As shown in the figure, two sets of data were close and the average error of 13 cities was 8%, the maximum gap reached 24% in Suzhou and Taizhou, the next reached 15% in Huai'an, others were under 10%. Overall, the model established in this paper was rational and feasible.

3 Results and Analysis

3.1 Projected precipitation and temperature

3.1.1 Temporal variations

Projected changes in precipitation, as calculated using the five models and three scenarios, showed that future precipitation will differ little from the base year, ranging from −7.7 to 10%; in contrast, the mean annual temperature over the next 30 years was predicted to increase by 0.81–1.82 °C (Fig. 9).

3.1.2 Spatial variations

Projected precipitation, simulated using the five models and three scenarios, showed an increasing trend generally,

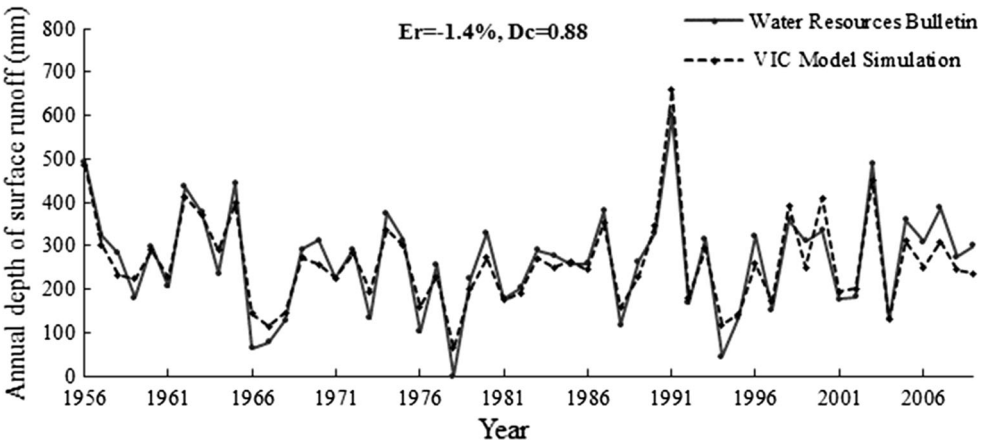

Fig. 6 Comparison of the 1956–2009 annual surface runoff depth (mm) simulated by the variable infiltration capacity (VIC) model (*dashed line*) and the values published by the Jiangsu Water Resources Bulletin (*solid line*). *Er* relative error, *Dc* annual runoff coefficient of determination

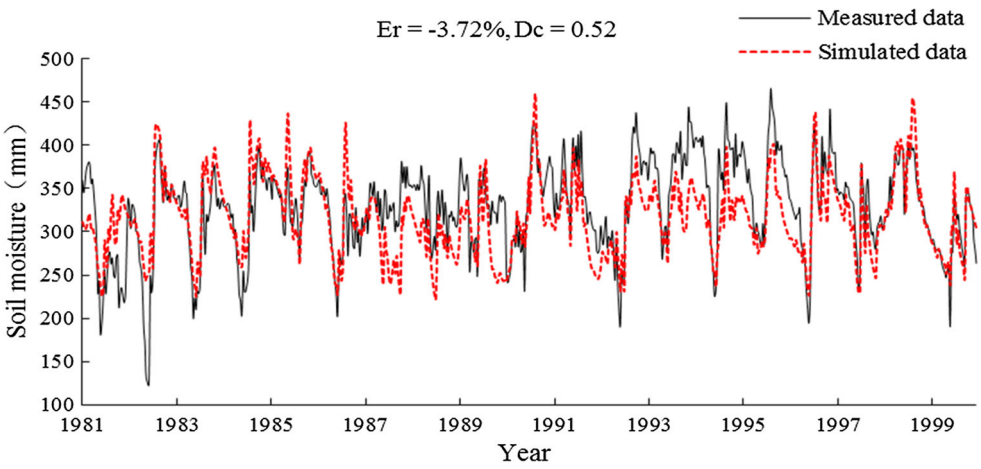

Fig. 7 Comparison of simulated (*red dashed*) and Measured (*black solid*) soil moisture (mm) for depths of 0–100 cm at Xuzhou station during 1981–1999. *Er* relative error, *Dc* coefficient of determination

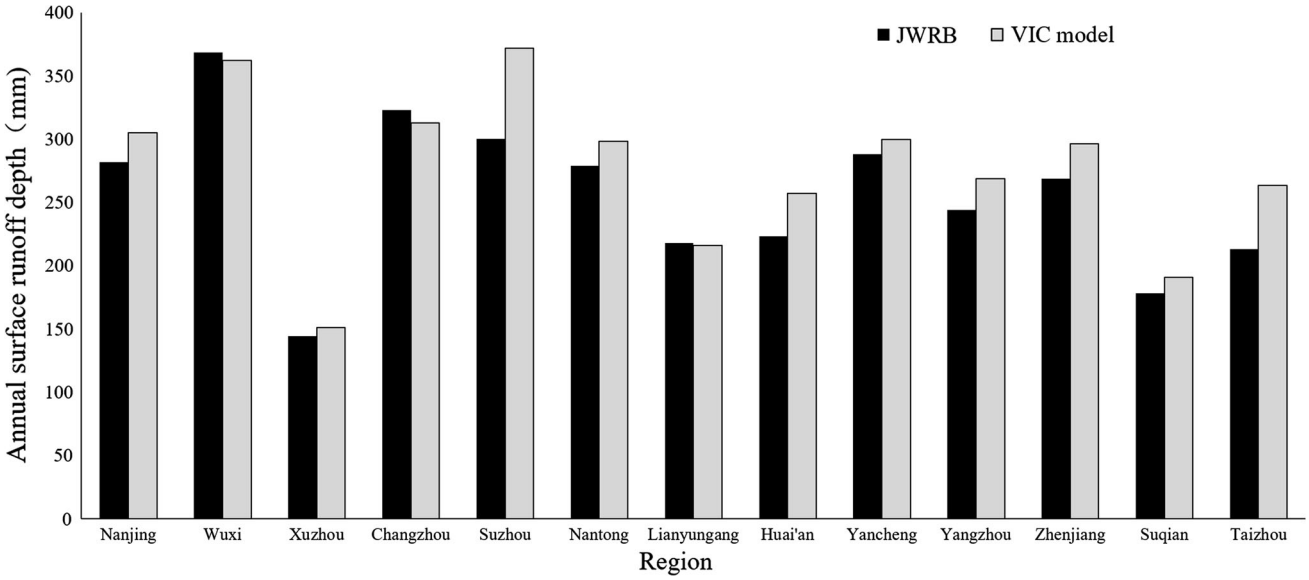

Fig. 8 Comparison of the 1980–2000 annual average surface runoff depth (mm) simulated by the VIC model (*grey bars*) and published by the Jiangsu Water Resources Bulletin of 13 cities (*black bars*)

with the rate of increase becoming gradually larger from south to north (Fig. 10a). Overall, precipitation in the Yishusi Basin was predicted to increase by more than 2%; although, western and eastern coastal regions increased 3–5%. In the Huaihe River Basin, precipitation was predicted to increase by 1–3%. In the Yangtze River and Taihu basins, potential increases were not obvious; although, in the southern part of the Taihu Basin, precipitation was predicted to decrease slightly. Projected temperatures in Jiangsu Province showed a significant increasing trend (Fig. 10b), with the rate of increase becoming gradually larger from southeast to northwest. Temperature was predicted to increase most significantly (by more than 1.32 °C per year) is the coastal border area between the Yishusi and Huaihe River basins.

3.2 Runoff changes over the next 30 years

3.2.1 Seasonal changes

Figure 11 showed the future (2010–2040) relative changes of monthly runoff depths compared with reference period (1970–1999) under RCP2.6, RCP4.5 and RCP8.5 scenarios. The histogram represented the average forecast results of five models and the error lines represented the variation range of five models. As can be seen that the relative

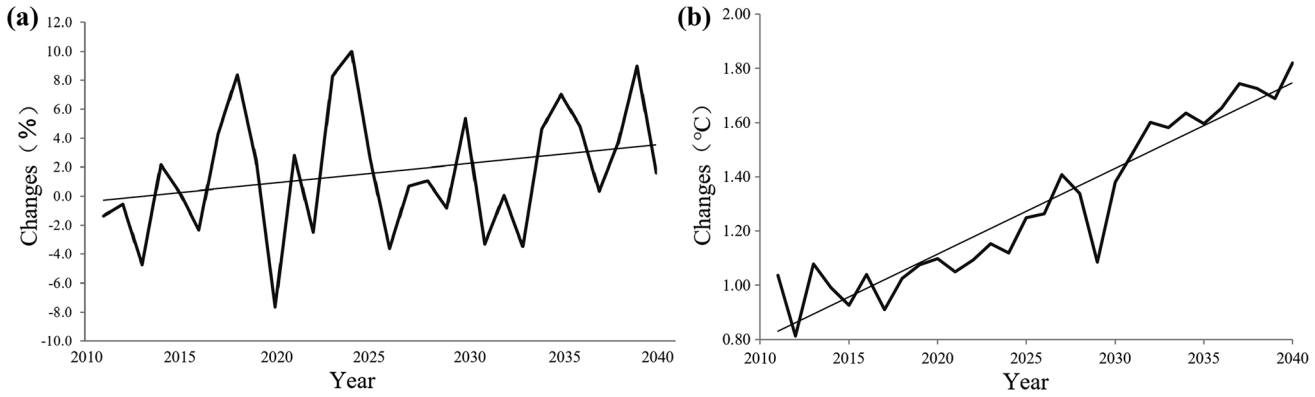

Fig. 9 The change trends of Annual mean precipitation (**a**) and temperature (**b**) in Jiangsu Province during 2011–2040 based on the results of five models (CCSM4, CSIRO-Mk3-6-0, GISS-E2-R, HadGEM2-ES, and IPSL-CM5A-LR) and three Representative Concentration Pathway (RCP) scenarios (2.6, 4.5, 8.5)

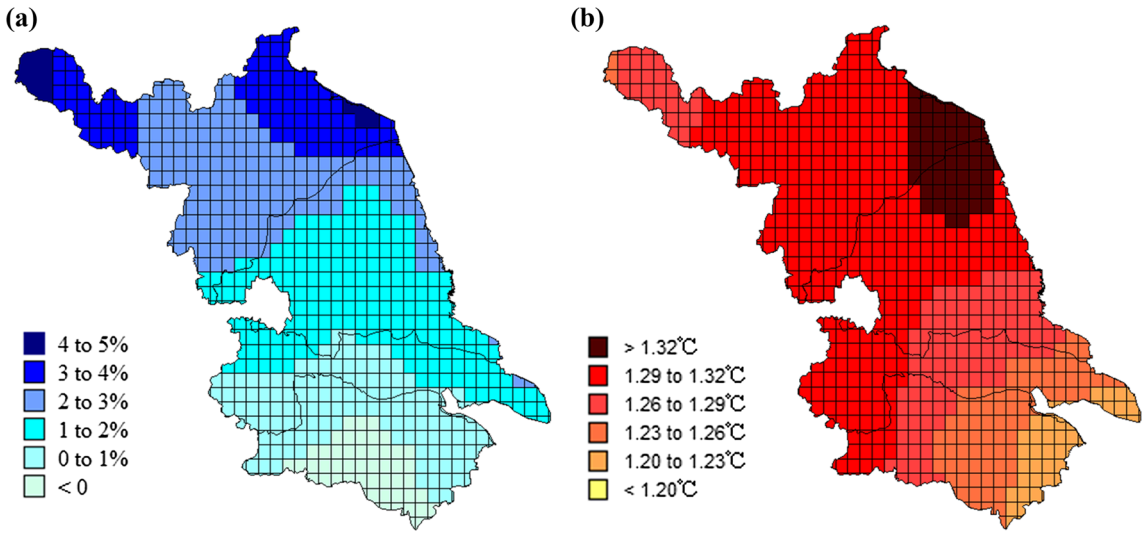

Fig. 10 Spatial variations in annual mean precipitation (**a**) and temperature (**b**) for Jiangsu province during 2011–2040 based on the results of five models (CCSM4, CSIRO-Mk3-6-0, GISS-E2-R, HadGEM2-ES, and IPSL-CM5A-LR) and three Representative Concentration Pathway (RCP) scenarios (2.6, 4.5, 8.5)

changes of monthly runoff depths showed large difference under three scenarios. The average runoff depths of five models tended to decrease in February, October and November, while the other months mainly tended to increase. The relative change range of runoff depths in December was from 44 to 75%, while other months were from −20 to 15%. As can be seen from the error lines under three scenarios, the consistency of predicted changes of five models was poor and the results still had great uncertainty, such as the ranges of monthly runoff depths in January under three scenarios were −52.21 to 52.84% (RCP2.6), −22.93 to 26.38% (RCP4.5) and −20.94 to 68.42% (RCP8.5), while the average changes were −9% (RCP2.6), −2% (RCP4.5) and 10% (RCP8.5).

3.2.2 Spatial variations

The predicted changes in the annual mean runoff of Jiangsu Province from 2011 to 2040 differed both spatially and temporally according to the model and RCP scenario employed (Figs. 12, 13, 14; Table 5). Under RCP2.6, model CCSM4 showed the most widespread and significant positive changes, while model GISS-E2-R consistently predicted reductions in runoff across the province (Fig. 12). Model GISS-E2-R also predicted widespread reductions in annual mean runoff depths under both RCP4.5 (Fig. 13) and RCP8.5 (Fig. 14). Under RCP4.5, only model HadGEM2-ES predicted consistent increases in runoff depth across the province, with the other models

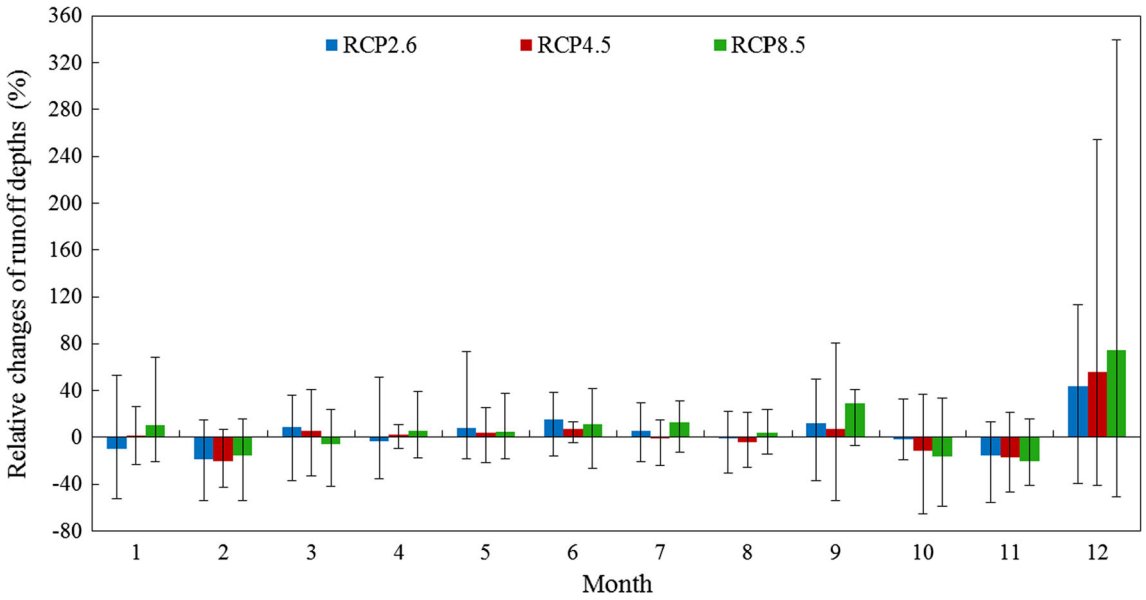

Fig. 11 Relative changes (%) of monthly runoff depths in the future (2011–2040) compared with reference period (1970–1999) under three scenarios in Jiangsu Province. The *colored bars* are the average results of five models (CCSM4, CSIRO-Mk3-6-0, GISS-E2-R, HadGEM2-ES, and IPSL-CM5A-LR) under three scenarios: RCP2.6 (*blue bars*), RCP 4.5 (*red bars*), and RCP 8.5 (*green bars*). Error lines represent the change range of five models

predicting both increases and decreases, depending on location. The most significant changes in runoff depth were predicted under RCP8.5 (Fig. 14). Changes in the Yishusi Basin showed an increasing trend in model CCSM4, HadGEM2-ES and IPSL-CM5A-LR under RCP2.6 and RCP4.5, in model CCSM4, CSIRO-Mk3-6-0 and HadGEM2-ES under RCP8.5. While changes in the Taihu Basin showed a decreasing trend in model GISS-E2-R and IPSL-CM5A-LR under three RCPs, HadGEM2-ES under RCP2.6 and CCSM4 under RCP4.5. The Huaihe River and Yangtze River basins contained both increasing and decreasing runoff depth predictions.

By averaging the results of the five models, our results predicted that overall, and for all three scenarios, runoff depths in the northern part of Jiangsu Province will follow a clear increasing trend over the next 30 years, while runoff depths may reduce slightly in the south (Fig. 15a). An analysis of the likelihood of an increasing trend (Fig. 15b; Table 6) supported this result, with the highest probability of increasing runoff depth occurring in the northern parts of the province. The annual mean runoff variation for the four basins under the three scenarios over the next 30 years ranged from approximately −6 to 15%. Overall, the annual mean runoff depths in the Taihu Basin were predicted to change by −6 to 3%, the Yangtze River and Huaihe River basins were predicted to increase by 0–12%, and the runoff depths in the Yishusi Basin were predicted to increase by 6–15%.

Based on RCP2.6 alone, runoff depths in the Taihu Basin may fall in the future, with the decreases predicted to be less than 3%, while the runoff depths in the other river basins were predicted to increase by 3–12%. Under RCP4.5, the runoff depths in the Taihu and Yangtze River basins were predicted to fall by −6 to −3%, while those of the Yishusi and Huaihe River basins were shown to be more likely to increase, with the increases predicted to be in the range of 0–3 and 6–9%, respectively. Under RCP8.5, the runoff depth in the Yishusi Basin was predicted to increase by 12–15%. The runoff depths in the other three basins were also shown to be likely to increase, in general by 3–12%; although, the increase in the Taihu Basin was predicted to be less than 3%.

4 Discussion

The results of this study highlight the different possible responses of runoff depth in Jiangsu Province to different forecasted climate change scenarios. The results contain some uncertainty, which mainly arises from: (1) the selection of the climate models and the uncertainty within the climate scenarios. In particular, while simulations of current climate may be good, there may be some errors for future climate simulations; (2) error within the VIC model used to simulate runoff. While the simulated runoff data were shown to closely match the data of the Jiangsu Province Water Resources Bulletin, deviations from actual

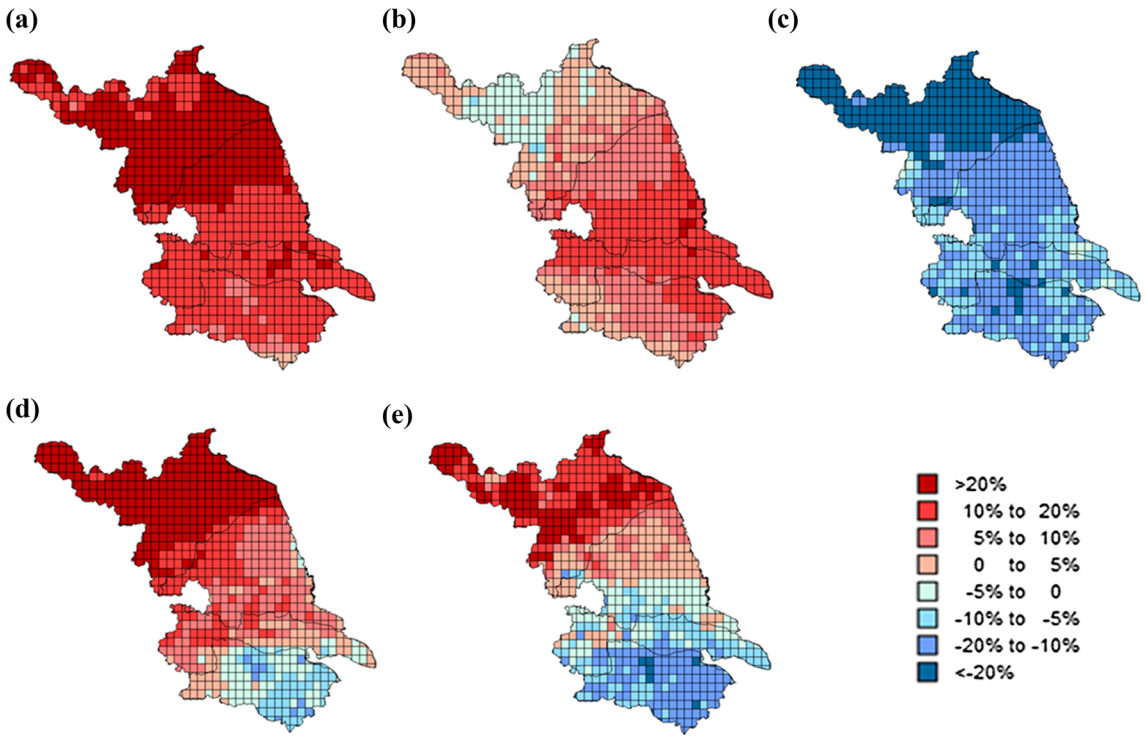

Fig. 12 Spatial variations in the relative change of annual mean runoff depth (%) in Jiangsu Province from 2011 to 2040 using the Representative Concentration Pathway (RCP) 2.6 scenario and models **a** CCSM4, **b** CSIRO-Mk3-6-0, **c** GISS-E2-R, **d** HadGEM2-ES, and **e** IPSL-CM5A-LR

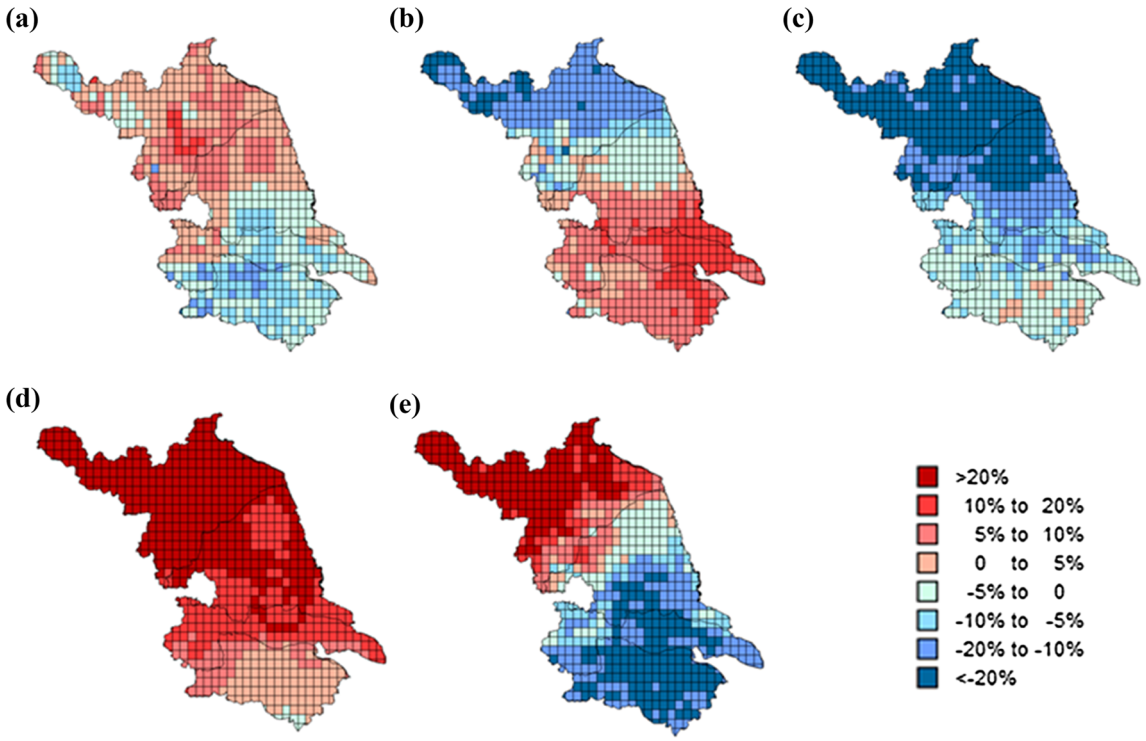

Fig. 13 The same as Fig. 12, but for RCP 4.5

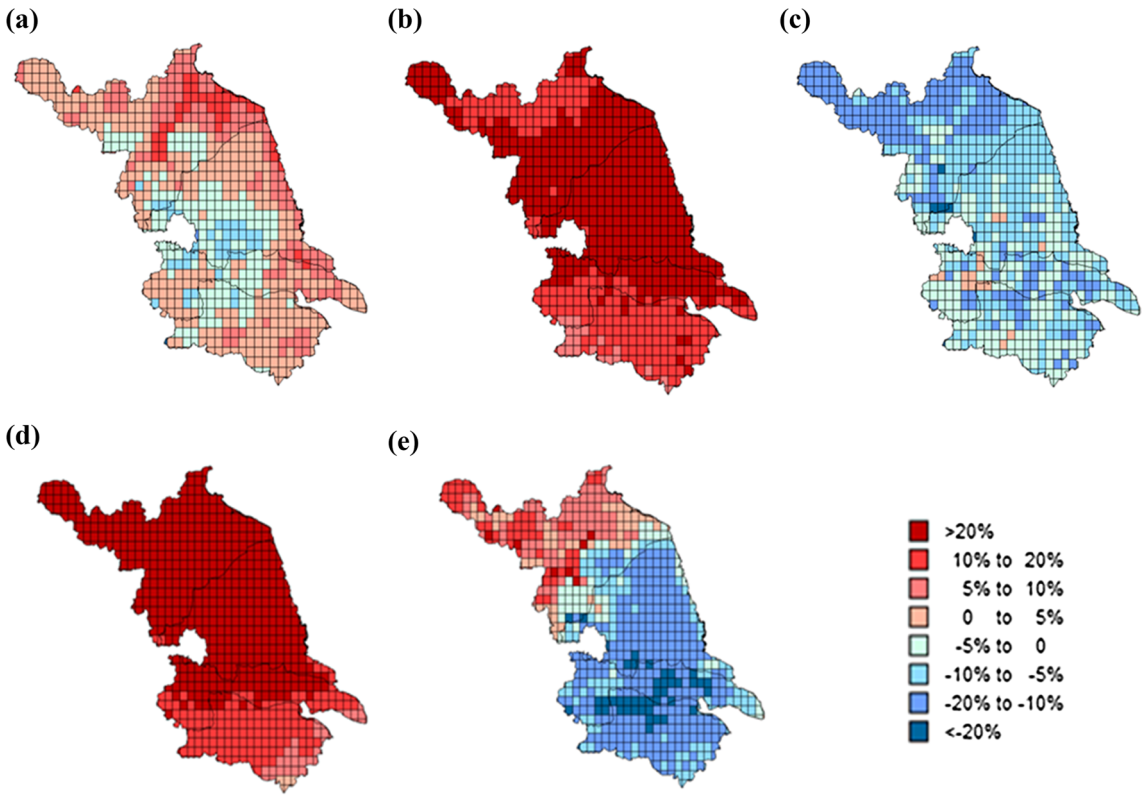

Fig. 14 The same as Fig. 12, but for RCP 8.5

Table 5 Relative changes (%) in annual mean runoff depths in the Jiangsu basins (2011–2040)

Model	Emissions scenario	Region			
		Yishusi Basin	Huaihe River Basin	Yangtze River Basin	Taihu Basin
CCSM4	RCP2.6[a]	25.4	19.0	15.4	11.1
	RCP4.5	4.1	1.7	−1.7	−5.7
	RCP8.5	4.7	1.5	1.5	2.1
CSIRO-Mk3-6-0	RCP2.6	2.1	11.9	11.6	6.3
	RCP4.5	−12.4	3.6	9.2	7.3
	RCP8.5	23.0	26.5	20.5	14.0
GISS-E2-R	RCP2.6	−23.9	−12.8	−9.9	−11.7
	RCP4.5	−24.1	−15.0	−5.0	−2.8
	RCP8.5	−9.9	−6.2	−5.6	−5.4
HadGEM2-ES	RCP2.6	33.9	9.5	4.7	−3.8
	RCP4.5	38.8	20.3	12.9	3.4
	RCP8.5	41.6	31.7	18.8	12.1
IPSL-CM5A-LR	RCP2.6	16.0	1.3	−6.1	−12.5
	RCP4.5	24.8	−7.2	−15.7	−22.4
	RCP8.5	4.6	−11.3	−11.7	−13.1

[a] *RCP* representative concentration pathway (i.e., greenhouse gas emissions scenarios)

runoff may still occur. However, despite these uncertainties, we believe the climate change trends simulated in this study to be highly accurate. Furthermore, our results are consistent with related research studies, which have shown that: (1) runoff in the Huaihe River Basin may increase from 2011 to 2060 (Zhang et al. 2014); (2) the runoff in the flood season may increase, while non-flood season runoff may decrease in the Yangtze River Basin (Ju et al. 2011),

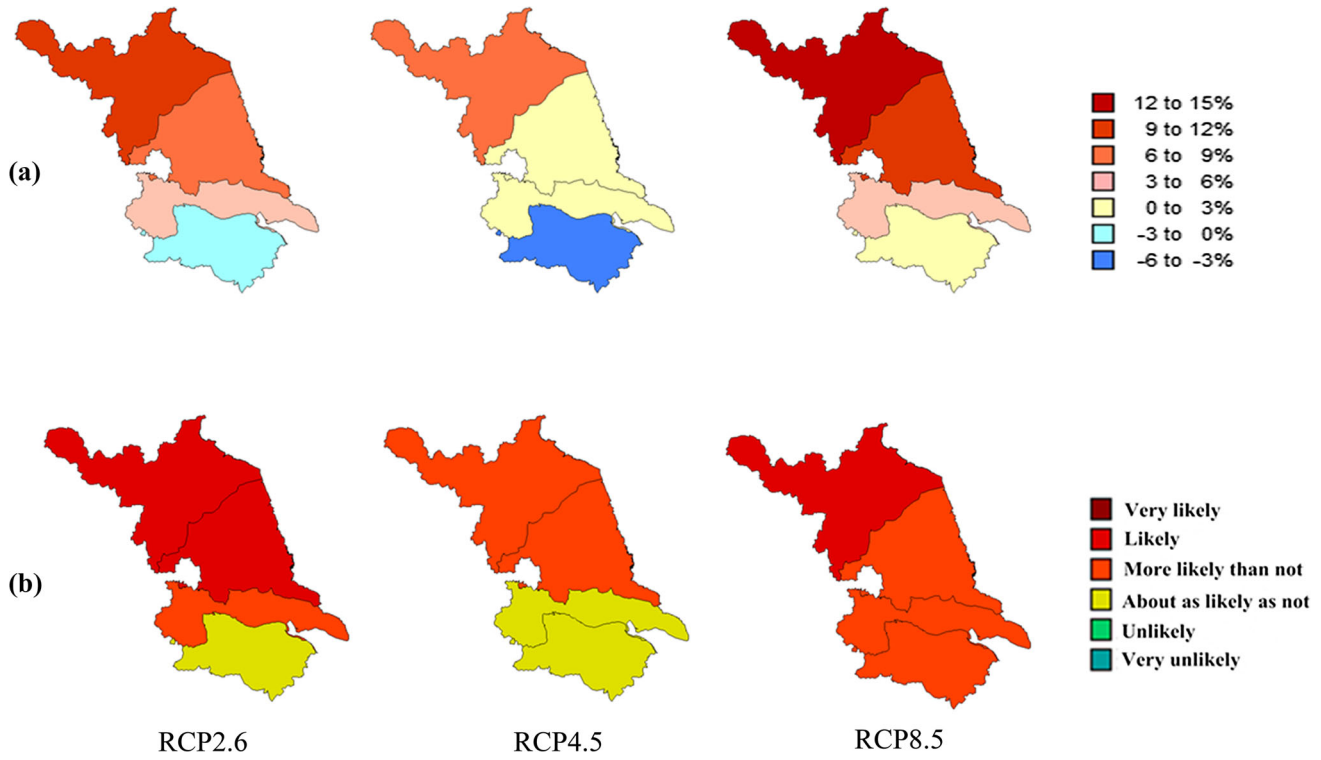

Fig. 15 Mean relative change in annual mean runoff depths and level of increased likelihood. **a** Mean relative change (%) in annual mean runoff depths and **b** the level of increased likelihood (*deep red* very likely; *light red* likely; *orange* more likely than not; *yellow* about as likely as not; *light green* unlikely; *deep green* very unlikely) in four watersheds using three Representative Concentration Pathway (RCP) scenarios (2.6, 4.5, 8.5) from 2011 to 2040

Table 6 Definitions of estimated result possibilities

Term	Model consistency
Very likely	Five model results are consistent
Likely	Four model results are consistent
More likely than not	Three model results are consistent
About as likely as not	Two model results are consistent
Unlikely	In contrast with 'Likely'
Very unlikely	In contrast with 'Very likely'

and; (3) from 2021 to 2050, the Taihu Basin runoff will increase, especially during flood seasons (Liu et al. 2010).

The predicted changes in Jiangsu Province surface runoff between 2011 and 2040 will have a significant impact on Jiangsu Province and it is critical that responses to these changes be considered. In particular: (1) the Yishusi Basin is the most water-stressed area of Jiangsu Province and its flood control engineering requirements are currently low; however, we should consider how future increases in runoff may increase flood challenges, and how flooding may impact on water quality; (2) While runoff in the Yangtze River Basin will likely increase in the future, it remains important to consider flood control during droughts and during the non-flood season. In particular, regional flooding or droughts may impact upon agricultural production; (3) Increasing runoff in the Huaihe River basin may exacerbate flooding. Polluted water from flood discharge will result in water environmental problems and may have an extremely negative effect on the quality of drinking water and on fishery production; (4) Higher predicted temperatures will seriously impact on the water environment, and may cause an increase in the series blue-green algae problems (Shang et al. 2010; Xie et al. 2016) suffered in the Taihu Basin. Furthermore, cyanobacteria stench and toxins may seriously affect the living environment of aquatic organisms and human life.

5 Summary and Conclusions

In this study, we used the VIC model to simulate Jiangsu Province runoff from 2011 to 2040, and by employing five CMIP5 global climate models, we were able to assess the impact of climate change on predicted runoff. The main findings of this study showed that:

(1) Annual mean precipitation under the five models and three scenarios showed a fluctuating upward trend, as compared with the reference period (1970–1999),

and ranged between −7.7 and 10%. The rate of increase was shown to become gradually larger from south to north, except in the southern part of the Taihu Basin, which showed a slight decrease.

(2) Annual mean temperature was projected to increase between 2011 and 2040, as compared with the reference period (1970–1999), with predicted increases ranging from 0.8–1.8 °C. Temperature increases were particularly pronounced after 2030. The rate of increase was shown to become gradually larger from southeast to northwest, with the largest rise in temperature predicted to be 1.34 °C.

(3) Increasing runoff depths were highest under the RCP8.5 emission scenario and lowest under RCP4.5. With the exception of February, October, November (where runoff depths were predicted to fall significantly between 2011 and 2040), monthly mean runoff depths were predicted to increase, with the most significant increases occurring in December.

(4) Spatial distributed runoff depths variations ranged from −6 to 12%. The likelihood of increasing runoff depths in the four basins increased from south to north. The largest increases in runoff depths were predicted by RCP8.5. Based on both RCP4.5 and RCP2.6, runoff depths in the Taihu Basin may see future reductions, but that in the other three basins were predicted to increase.

The predicted changes in runoff depth in Jiangsu Province will have significant implications for flood management, agricultural production, fisheries, water resource security, water quality, and the heath of aquatic ecosystems; therefore, the results of this study will provide an important reference for policymakers planning for the future water resources of Jiangsu Province. Furthermore, we conducted a case study with the VIC model, it showed high consistency with measured values and provides new reference values for the study of other plain regions, for which the underlying conditions are very complex.

Acknowledgements This study was funded by the Natural Science Foundation of Jiangsu Province of China (Grant No. BK20131368), the National Natural Science Foundation of China (Grant No. 51579065), the Foundation for the Author of National Excellent Doctoral Dissertation of P.R. China (Grant No. 201161) and the Program for New Century Excellent Talents in University (Grant No. NCET-12-0842).

References

Chang JX, Wang YM, Istanbulluoglu E, Bai T, Huang Q, Yang DW, Huang SZ (2014) Impact of climate change and human activities on runoff in the Weihe River Basin, China. Q Int 380–381:169–179. doi:10.1016/j.quaint.2014.03.048

Chen FW, Li CW (2012) Estimation of the spatial rainfall distribution using inverse distance weighting (IDW) in the middle of Taiwan. Paddy Water Environ 10(3):209–222. doi:10.1007/s10333-012-0319-1

Deng ZW, Zhou XL, Chen HS (2004) Spatial variation of precipitation trend and interdecadal change in Jiangsu. Meteorological 6:696–705

Dufresne JL, Foujols MA, Denvil S, Caubel A, Marti O, Aumont O, Balkanski Y, Bekki S, Bellenger H, Benshila R, Bony S, Bopp L, Braconnot P, Brockmann P, Cadule P, Cheruy F, Codron F, Cozic A, Cugnet D, de Noblet N, Duvel JP, Ethé C, Fairhead L, Fichefet T, Flavoni S, Friedlingstein P, Grandpeix JY, Guez L, Guilyardi E, Hauglustaine D, Hourdin F, Idelkadi A, Ghattas J, Joussaume S, Kageyama M, Krinner G, Labetoulle S, Lahellec A, Lefebvre MP, Lefevre F, Levy C, Li ZX, Lloyd J, Lott F, Madec G, Mancip M, Marchand M, Masson S, Meurdesoif Y, Mignot J, Musat I, Parouty S, Polcher J, Rio C, Schulz M, Swingedouw D, Szopa S, Talandier C, Terray P, Viovy N, Vuichard N (2013) Climate change projections using the IPSL-CM5 Earth System Model: from CMIP3 to CMIP5. Clim Dyn 40(9–10):2123–2165. doi:10.1007/s00382-012-1636-1

Fu YY, Yang XQ, Shen W (2013) Interdecadal variations and the correlation analysis of temperature and precipitation during winter in Jiangsu Province. J Meteorol Sci 2:178–183

Gosling SN, Taylor RG, Arnell NW, Todd MC (2011) A comparative analysis of projected impacts of climate change on river runoff from global and catchment-scale hydrological models. Hydrol Earth Syst Sci 15:279–294. doi:10.5194/hess-15-279-2011

Gu WL, Wang JF, Zhu LL (2010) Changes in precipitation and water resources in Henan Province in 1956–2007. Adv Clim Change Res 6(4):277–283

IPCC (2012) Managing the risks of extreme events and disasters to advance climate change adaptation. A special report of working Groups I and II of the intergovernmental panel on climate change. Cambridge University Press, Cambridge

IPCC (2013) Climate change 2013: the physical science basis. Cambridge University Press, Cambridge

Ju Q, Hao ZC, Yu ZB, Xu HQ, Jiang WJ, Hao J (2011) Runoff prediction in the Yangtze River basin based on IPCC AR4 climate change scencrios. Adv water Sci 22(4):462–469

Kusangaya S, Michele LW, Emma AvG, Graham PWJ (2014) Impacts of climate change on water resources in southern Africa: a review. Phys Chem Earth 67–69:47–54. doi:10.1016/j.pce.2013.09.014

Lespinas F, Ludwig W, Heussner S (2014) Hydrological and climatic uncertainties associated with modeling the impact of climate change on water resources of small Mediterranean coastal rivers. J Hydrol 511(4):403–422. doi:10.1016/j.jhydrol.2014.01.033

Li X, Cheng GD, Lu L (2000) Comparison of spatial interpolation method. Adv Earth Sci 15(3):260–265. doi:10.11867/j.issn.1001-8166.2000.03.0260

Li Z, Liu WZ, Zhang XC, Zheng FL (2010) Assessing and regulating the impacts of climate change on water resources in the Heihe watershed on the Loess Plateau of China. Sci China 5:710–720. doi:10.1007/s11430-009-0186-9

Liang X, Wood EF, Lettenmaier DP (1996) Surface soil moisture parameterization of the VIC–2L model: evaluation and modification. Glob Planet Change 13(1):195–206. doi:10.1016/0921-8181(95)00046-1

Liu M, Wei JS, Yu JW, Zhang B (2009) The temporal-spatial distribution climatic feature of thunderstorm day number in Jiangsu province about 57 a. Sci Meteorol Sin 6:827–832

Liu L, Xu ZX, Huang JX (2010) Impact of climate change on runoff in the Taihu basin. J Beijing Normal Univ 3:371–377

Lu GY, Wong DW (2008) An adaptive inverse-distance weighting spatial interpolation technique. Comput Geosci 34(9):1044–1055. doi:10.1016/j.cageo.2007.07.010

Lu GH, Wu ZY, He H (2010) Hydrological cycle and quantitative forecast. Science Press, Beijing

Lu GH, Zhang J, Wu ZY, He H (2013) Parameter gridding formulas of VIC Model in southern region of China and effect verification. Water Resour Power 5:13–17

Lu GH, Yang Y, Wu ZY, He H, Xiao H (2014) Temporal and spatial variations of snow depth in regions of the upper reaches of Yangtze River under future climate change scenarios: a study based on CMIP5 multi-model ensemble projections. Adv Water Sci 6(4):484–493

Ma Q (2007) Evaluation and utilization of surface water resources in Jiangsu Province. China Rural Water Hydropower 11:74–76

Madsen H, Lawrence D, Lang M, Martinkova M, Kjeldsen TR (2014) Review of trend analysis and climate change projections of extreme precipitation and floods in Europe. J Hydrol 519:3634–3650. doi:10.1016/j.jhydrol.2014.11.003

Pennell C (2010) On the effective number of climate models. University of Utah, Salt Lake City

Qiu XF, Zhang XL, Zeng Y, Wu JG (2008) Precipitation variation trend in Jiangsu Province from 1961 to 2005. Meteorol Mon 34(5):82–88

Shu C, Liu SX, Mo XG, Liang ZM, Dai D (2008) Uncertainty analysis of Xinanjiang model parameter. Geogr Res 27(2):343–352. doi:10.3321/j.issn:1000-0585.2008.02.012

Sivakumar B (2011) Global climate change and its impacts on water resources planning and management: assessment and challenges. Stoch Env Res Risk Assess 25(4):583–600. doi:10.1007/s00477-010-0423-y

Spinoni J, Naumann G, Jürgen VV, Barbosa P (2015) The biggest drought events in Europe from 1950 to 2012. J Hydrol 3:509–524. doi:10.1016/j.ejrh.2015.01.001

Shang ZT, Ren J, Qin MR, Xia Y, He L, Chen YW (2010) The relationship between climatic change and blue algae eruption in Taihu Lake. Chin J Ecol 1:55–61. doi:10.13292/j.1000-4890.2010.0047

Sun Y, Yin DP, Zong PS (2013a) Climate characteristics of freezing disaster in Jiangsu. J Nat Disast 2:165–171

Sun JL, Lei XH, Tian Y, Liao WH, Wang YH (2013b) Hydrological impacts of climate change in the upper reaches of the Yangtze River Basin. Q Int 304(447):62–74. doi:10.1016/j.quaint.2013.02.038

Tezuka S, Takiguchi H, Kazama S, Sato A, Kawagoe S, Sarukkalige R (2014) Estimation of the effects of climate change on flood-triggered economic losses in Japan. Int J Disast Risk Reduct 9(1):58–67. doi:10.1016/j.ijdrr.2014.03.004

The office of Jiangsu province water resource comprehensive planning leading group (2014) Investigation and assessment of water resources in Jiangsu province. Jiangsu Province Hydrology and Water Resources Investigation Bureau 10

Vaghefi SA, Mousavi SJ, Abbaspour KC, Srinivasan R, Yang H (2014) Analyses of the impact of climate change on water resources components, drought and wheat yield in semiarid regions: Karkheh River Basin in Iran. Hydrol Process 28(4):2018–2032. doi:10.1002/hyp.9747

Wang GQ, Zhan JY (2015) Variation of water resources in the Huang-huai-hai areas and adaptive strategies to climate change. Q Int 1–7. doi:10.1016/j.quaint.2015.02.005

Wang XY, Yang T, Krysanova V, Yu ZB (2015a) Assessing the impact of climate change on flood in an alpine catchment using multiple hydrological models. Stoc Env Res Risk Assess 29(8):2143–2158. doi:10.1007/s00477-015-1062-0

Wang WG, Wei JD, Shao QX, Xing WQ, Yong B, Yu ZB, Jiao XY (2015b) Spatial and temporal variations in hydro-climatic variables and runoff in response to climate change in the Luanhe River basin, China. Stoch Env Res Risk Assess 29(4):1117–1133. doi:10.1007/s00477-014-1003-3

Wu ZY, Guo HL, Jin JL, Yan GX (2010) Extreme hydrologic event response to climate change scenario in Heihe Basin. Water Resource Power 28(2):7–9

Xia L, Zhang Q, Sun N, Zhai YJ, Wang SH (2014) Nearly 53 years of climate changes analysis in Jiangsu province. Chinese Meteorological Society 31th Annual Meeting –S3 short-term climate prediction theories, methods and techniques, pp 149–161

Xie XP, Li YC, Hang X, Huang S (2016) The effect of air temperature on the process of cyanobacteria recruitment and dormancy in Lake Taihu. J Lake Sci 28(4):818–824. doi:10.18307/2016.0415

Xu CH, Xu Y (2012) The projection of temperature and precipitation over China under RCP Scenarios using a cmip5 multi-model ensemble. Atmos Ocean Sci Lett 5(6):527–533

Xu JJ, Yang DW, Yi YH, Lei ZD, Chen J, Yang WJ (2008) Spatial and temporal variation of runoff in the Yangtze River basin during the past 40 years. Q Int 186(1):32–42. doi:10.1016/j.quaint.2007.10.014

Yang H, Li CY (2003) The relation between atmospheric intraseasonal oscillation and summer severe flood and drought in the Changjiang-Huaihe River basin. Adv Atmos Sci 4:540–553

Zhang SF, Gu Y, Lin J (2010) Uncertainty analysis in the application of climate models. Adv Water Sci 21(4):504–511

Zhang ZT, Gao C., Zhai JQ, Jin GJ, Liu Q (2014) Observed (1958–2007) and projected (2011–2060) trends of climate change and streamflow in the Huaihe River basin, China. J Chuzhou Univ 4:10–14

Zhao ZC, Luo Y, Huang JB (2013) A review on evaluation methods of climate modeling. Adv Clim Change Res 5(4):241–243

Zorita E, von SH (1999) The analog method as a simple statistical downscaling technique: comparison with more complicated methods. J Clim 12(8):2474–2489. doi:10.1175/1520-0442(1999)012<2474:TAMAAS>2.0.CO;2